J|A|C|S ARTICLES

Published on Web 11/13/2009

Precise Characterization of the Conformation Fluctuations of Freely Diffusing DNA: Beyond Rouse and Zimm

Kevin McHale*,† and Hideo Mabuchi

Edward L. Ginzton Laboratory, Stanford University, Stanford, California 94305

Received August 17, 2009; E-mail: mchalekl@niddk.nih.gov

Abstract: We studied the dynamics of single freely diffusing fluorescence-labeled double-stranded λ-phage DNA molecules using dual-color 3-dimensional feedback tracking microscopy and intramolecular fluorescence correlation spectroscopy. Our technique is independently sensitive to the molecule's diffusion coefficient D and radius of gyration R_g and is concentration insensitive, providing greater precision for characterizing the molecule's intramolecular motion than other methods. We measured $D = 0.80 \pm 0.05$ $\mu m^2/s$ and $R_g \approx 420$ nm, consistent with the Kirkwood−Riseman prediction for a flexible polymer with strong hydrodynamic interactions (HI), but we find the statistics of intramolecular motion inconsistent with the Zimm model for such a polymer. We address a dispute in the experimental literature, finding that previous measurements on double-stranded DNA likely lacked the sensitivity to distinguish between the Zimm model and the HI-free Rouse model. Finally, we observe fluorescence fluctuations with a correlation time of over 2 s that cannot be explained by either model and propose that they may be signatures of excluded volume interactions.

The physics of polymer motion has broad implications throughout biomolecular science. From protein folding to DNA transcription and translation, the fundamental processes of biology are dictated by interactions within and between polymers. The dynamics of polymers in solution can be described precisely by equations of motion that incorporate the mechanical properties of the polymer, the thermal fluctuations of the solvent, and the hydrodynamic coupling between the two. These equations are nonlinear, so their analysis is difficult and relies on approximations for making quantitative predictions. The earliest such approximation was formulated by Rouse,[1] who simply neglected all nonlinearities to produce an equation of motion with an exact solution. Zimm[2] later incorporated hydrodynamic interactions (HI)—by which fluid flows induced by the motion of one region of the polymer influence the motion of spatially proximate regions—using a preaveraging approximation to preserve the model's linearity. Each of these approximations provides an estimate of the relationship between a polymer's length and its translational diffusion coefficient. Light scattering experiments have shown the Zimm prediction to be more accurate, so the Zimm model is commonly regarded as the better of the two.[3] However, these models also predict rich sets of intramolecular motions that cannot be measured by traditional scattering techniques due to poor sensitivity and specificity.

The first measurements of intramolecular polymer dynamics were made on DNA molecules stretched in optical tweezers[4] and shown to be consistent with a semiflexible polymer (with significant resistance to bending on short length scales) with strong HI.[5,6] More recently, fluorescence correlation spectroscopy (FCS)[7−9] was applied to freely diffusing dsDNA,[10−13] and image correlation analysis and principle component analysis were applied to DNA immobilized in a 2-dimensional electroosmotic trap.[14,15] These experiments produced conflicting conclusions: one suggested the absence of HI in the intramolecular dynamics,[11] while the rest suggested that HI dominate those dynamics.

As discussed in refs 13 and 16, the inappropriate application of approximate solutions to the Rouse and Zimm dynamics raises uncertainty over several of these conclusions.[10,11,14] We further argue in this paper that the FCS approach to this problem is ill posed: the FCS curves predicted by the Rouse and Zimm models contain enough free parameters to render the predictions indistinguishable to within reasonable experimental uncertainty. We used feedback-tracking microscopy combined with FCS (tracking-FCS or tFCS)[17−20] to mitigate this problem, reducing

† Current address: Laboratory of Chemical Physics, NIDDK, National Institutes of Health, Bethesda, MD 20892.

(1) Rouse, P. E., Jr. *J. Chem. Phys.* **1953**, *21*, 1272–1280.
(2) Zimm, B. H. *J. Chem. Phys.* **1956**, *24*, 269–278.
(3) Doi, M.; Edwards, S. F. *The Theory of Polymer Dynamics*; International Series of Monographs on Physics; Clarendon Press: Oxford, 1986.
(4) Quake, S. R.; Babcock, H.; Chu, S. *Nature* **1997**, *388*, 151–154.
(5) Winkler, R. G. *Phys. Rev. Lett.* **1999**, *82*, 1843–1846.
(6) Harnau, L.; Reineker, P. *New J. Phys.* **1999**, *1*, 3.13.6.
(7) Magde, D.; Elson, E.; Webb, W. W. *Phys. Rev. Lett.* **1972**, *29*, 705–708.
(8) Elson, E. L.; Magde, D. *Biopolymers* **1974**, *13*, 1–27.
(9) Krichevsky, O.; Bonnet, G. *Rep. Prog. Phys.* **2002**, *65*, 251–297.
(10) Lumma, D.; Keller, S.; Vilgis, T.; Rädler, J. O. *Phys. Rev. Lett.* **2003**, *90*, 218301.
(11) Shusterman, R.; Alon, S.; Gavrinyov, T.; Krichevsky, O. *Phys. Rev. Lett.* **2004**, *92*, 048303.
(12) Winkler, R. G.; Keller, S.; Rädler, J. O. *Phys. Rev. E* **2006**, *73*, 041919.
(13) Petrov, E. P.; Ohrt, T.; Winkler, R. G.; Schwille, P. *Phys. Rev. Lett.* **2006**, *97*, 258101.
(14) Cohen, A. E.; Moerner, W. E. *Phys. Rev. Lett.* **2007**, *98*, 116001.
(15) Cohen, A. E.; Moerner, W. *Proc. Natl. Acad. Sci. U.S.A.* **2007**, *104*, 12622–12627.
(16) Tothova, J.; Brutovsky, B.; Lisy, V. *Eur. Phys. J. E* **2007**, *24*, 61–67.
(17) Berglund, A. J.; Mabuchi, H. *Opt. Express* **2005**, *13*, 8069–8082.

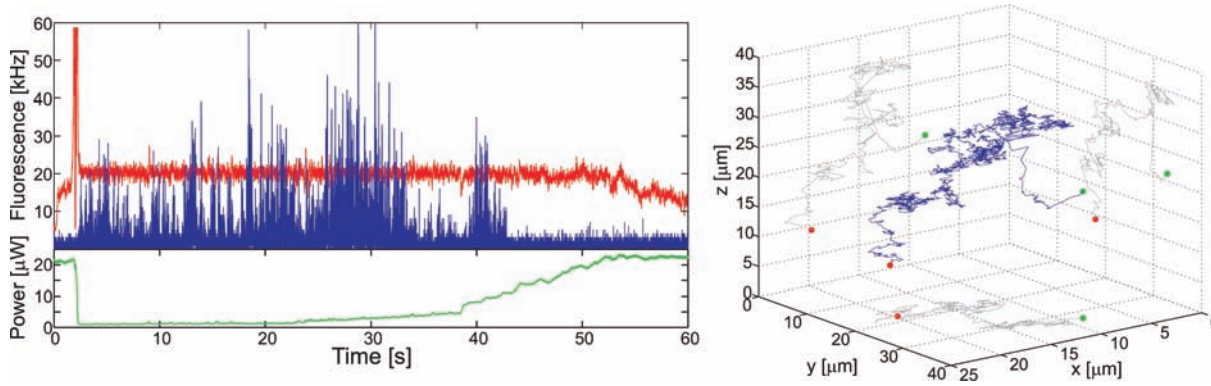

Figure 1. Example data from one DNA molecule. (Left, top) Fluorescence of the tracking (red) and probe (blue) dyes. Probe fluorescence is averaged over 1 ms bins, while tracking fluorescence is recorded as an analog signal with 17 Hz bandwidth. (Left, bottom) Tracking beam power. (Right) Position of the stage in three dimensions (blue) with projections (gray) into the *xy*, *xz*, and *yz* planes. Green and red circles indicate the beginning and end of the trajectory. 3-D trace and projections are sampled at 20 and 250 ms intervals, respectively.

the number of free parameters by one-half to provide independent quantitative estimates of all parameters in the polymer model. Furthermore, we monitored the dynamics of individual molecules over time scales as long as tens of seconds to look for deviations from the Rouse and Zimm theories, and we conclude that neither provides a fully satisfactory account of all our experimental observations.

Experimental Section

Feedback-tracking microscopy[21,22] refers to a set of techniques developed by several groups using a variety of related implementations.[23−31] In our approach,[17−20,26,32] spatially modulated laser beams and lock-in detection provide an estimate of the position of a fluorescence-labeled molecule in 3 dimensions, which we feed back to piezoelectric stages that move our microscope optics and sample to keep the molecule in focus. While tracking we record the positions of the stages, measured by calibrated capacitive sensors, and the arrival times of fluorescence photons, measured by avalanche photodiodes with nanosecond time resolution. We perform off-line analysis of the fluorescence signals using FCS. Tracking times range up to 1000 times longer than in a passive FCS experiment (limited by the travel of our stages), providing us with enough statistics to resolve complete FCS curves on single molecules and allowing us to probe correlations on time scales ranging up to the trajectory duration.

We used our instrument[19] to track fluorescence-labeled double-stranded λ-phage DNA (48 502 bp) for times ranging from 5 to 55 s. The molecules were labeled randomly along their backbones with several hundred of the intercalating dye POPO-3, which was excited at 532 nm by a tracking laser beam with a relatively large 1 μm waist to provide the signal for the tracking system. In addition, we incorporated a single Atto425 dye on one end of the molecule and probed this dye with a 444 nm laser beam focused into the tracking system's fixed point to a nearly diffraction-limited 280 nm waist. In this configuration the tracking beam is larger than the molecule, so the signal from the tracking dyes is dominated by the motion of the molecule's center of mass. By contrast, the probe beam is much smaller than the molecule, so that the signal from the probe dye is dominated by intramolecular motion.[10] Furthermore, positioning a single dye in a precise location on the molecule provides greater sensitivity to intramolecular motion than the alternative of placing multiple dyes in random positions (as with the tracking dyes), both because uncorrelated fluctuations in the motion of multiple dyes average to zero and because variations in the dye positions between molecules translate to detectable, systematic variations in the fluorescence statistics.[20]

We take several steps to prevent the loss of tracking fidelity due to photobleaching of the tracking dyes or the excitation of tracking dyes by the probe beam. First, we use a separate feedback system that dynamically adjusts the intensity of the tracking beam in real time to keep the fluorescence rate fixed at 20 kHz. When a molecule initially drifts into focus all of its dyes are intact, so the intensity required to achieve this fluorescence rate is fairly low. As the tracking dyes bleach, the feedback system increases the intensity, so that the fluorescence rate—and, therefore, the tracking fidelity—do not change. In addition, we monitor the beam intensity while acquiring data, and it provides us with information both for estimating the density of the POPO-3 labeling and for detecting collisions between molecules while tracking (see the Supporting Information; this system was first used in ref 32).

Second, although the probe beam's wavelength is far from the resonance of the tracking dyes, its intensity is high enough to induce a significant amount of fluorescence from them. To prevent this from adding noise to the tracking system, we alternate the excitation of the molecule so that the tracking and probe beams are never simultaneously turned on. The tracking system only operates when the tracking beam is on, so all probe-induced fluorescence is invisible to it. Provided we use a frequency much larger than the tracking bandwidth, this alternation does not affect the tracking system (see the Supporting Information). It does, however, induce a large oscillation in the tFCS curves that we correct for in our fits (see the Supporting Information).

More details regarding the instrument and sample preparation procedure are described in the Supporting Information.

Results

Example data is shown in Figure 1. A molecule drifts into the vicinity of the tracking stage, which jumps 10 μm vertically

(18) Berglund, A. J.; McHale, K.; Mabuchi, H. *Opt. Express* **2007**, *15*, 7752–7773.
(19) McHale, K.; Berglund, A. J.; Mabuchi, H. *Nano Lett.* **2007**, *7*, 3535–3539.
(20) McHale, K.; Mabuchi, H. Submitted for publication, 2009. arXiv: 0908.1177.
(21) Moerner, W. E. *Proc. Natl. Acad. Sci. U.S.A.* **2007**, *104*, 12596–12602.
(22) Cang, H.; Xu, C. S.; Yang, H. *Chem. Phys. Lett.* **2008**, *457*, 285–291.
(23) Berg, H. C. *Rev. Sci. Instrum.* **1971**, *42*, 868.
(24) Enderlein, J. *Appl. Phys. B: Laser Opt.* **2000**, *71*, 773–777.
(25) Levi, V.; Ruan, Q.; Kis-Petikova, K.; Gratton, E. *Biochem. Soc. Trans.* **2003**, *31*, 997–1000.
(26) Berglund, A. J.; Mabuchi, H. *App. Phys. B.* **2004**, *78*, 653.
(27) Cohen, A. E.; Moerner, W. E. *Appl. Phys. Lett.* **2005**, *88*, 223901.
(28) Andersson, S. B. *Appl. Phys. B: Laser Opt.* **2005**, *80*, 809.
(29) Lessard, G. A.; Goodwin, P. M.; Werner, J. H. *Proc. SPIE* **2006**, *6092*, 609205.
(30) Chaudhary, S.; Shapiro, B. *IEEE Trans. Control Syst. Technol.* **2006**, *14*, 669–680.
(31) Cang, H.; Wong, C. M.; Xu, C. S.; Rizvi, A. H.; Yang, H. *Appl. Phys. Lett.* **2006**, *88*, 223901.
(32) Berglund, A. J.; McHale, K.; Mabuchi, H. *Opt. Lett.* **2007**, *32*, 145–147.

to begin tracking it. The tracking fluorescence rate increases rapidly, and the intensity feedback responds by attenuating the beam. The molecule is tracked for over 60 s, but the probe dye bleaches after about 40 s, and the tracking dyes become too sparse to maintain the target fluorescence rate after about 50 s. We should note that the data in the figure was not used in our tFCS analysis. We restricted our analysis to data taken with lower (by a factor of 2) probe beam intensity in order to suppress light-induced nonlinearities in the dye fluorescence as much as possible.

Center-of-Mass Statistics and Tracking Errors. A powerful feature of feedback-tracking experiments is that the molecule's diffusion coefficient D can be estimated directly from the tracking stage motion, which is completely decoupled from the Atto425 fluorescence statistics. However, no feedback system can perfectly track any molecule's Brownian motion because doing so would require an infinite signal-to-noise ratio and feedback bandwidth.[32,33] As a consequence, the motion of the tracking stage represents an imperfect estimate of the molecule's trajectory. We must characterize this imprecision accurately because it adds systematic artifacts both to estimates for D and to the measured tFCS curves that must not be interpreted as part of the molecule's dynamic behavior.

A detailed model describing the tracking stage dynamics and a method for extracting the model parameters from the stage statistics were introduced in ref 18. In brief, we compute the variance of the increment of the stage positions as a function of the increment interval τ and scale it by $(2\tau)^{-1}$, so that the result is an estimate of the molecule's diffusion coefficient over intervals of length τ

$$\hat{D}(\tau) = (2\tau)^{-1}\mathrm{Var}[y(t+\tau) - y(t)] \tag{1}$$

where $y(t)$ is the position of one of the stages at time t and the variance is computed as an average over t. For intervals τ shorter than the inverse feedback bandwidth, $\hat{D}(\tau)$ is small because of latency in the stage response. For larger τ, $\hat{D}(\tau)$ asymptotically approaches its value for true Brownian motion, D. An exact functional form for $\hat{D}(\tau)$ can be found for any linear feedback system, and the model parameters—including the feedback bandwidth and localization noise density—may be extracted by fitting to the data. From these parameters we compute a measure of tracking error, $\sigma^2 = \langle[y(t) - x_{\mathrm{cm}}(t)]^2\rangle$, where $x_{\mathrm{cm}}(t)$ is the molecule's center of mass.

We tracked the λ-phage DNA molecules with feedback bandwidths $\gamma = 15$ Hz on the x and y axes and 2 Hz on the z axis. These corresponded to tracking errors $\sigma = 100$, 120, and 290 nm on the three axes, respectively, where the difference between the x and y axes is due to differences in localization noise. We determined the diffusion coefficient of this molecule to be $D = 0.80 \pm 0.05$ μm^2/s. The fit curves and more details are contained in the Supporting Information.

Intramolecular Tracking-FCS. We now analyze the fluorescence signal from the Atto425 probe dye. The Rouse and Zimm models both describe a Gaussian polymer without coupling between orthogonal Cartesian axes. By approximating the excitation beam with a 3-dimensional Gaussian, the tFCS curve for these models factorizes into a product of three curves—one for each axis—with identical functional forms. For the x axis, we have[20]

$$g_x(\tau) = \left[1 - \left(\frac{\sigma_x^2 e^{-\gamma_x \tau} + \frac{1}{3}\langle r^{t+\tau}\cdot r^t\rangle}{\sigma_x^2 + \frac{1}{3}r_0^2 + \frac{1}{4}w_x^2}\right)^2\right]^{-1/2} \tag{2}$$

where σ_x is the tracking error defined in the previous section and γ_x is the tracking bandwidth, r^t is the vector position of the dye at time t, $r_0^2 = \langle|r^t|^2\rangle$ is the mean-squared distance between the dye and the molecule's center of mass, and w_x is the waist of the beam. We must further account for two systematic components of the tFCS curve. First, alternating excitation induces periodic oscillations that we denote $g_{\mathrm{ae}}(\tau)$ and derive in the Supporting Information. Second, the background fluorescence (averaging 370 photons/s) attenuates the measured tFCS curve by a factor $g_{\mathrm{b}} = 1/(1+\kappa_1)(1+\kappa_2)$, where κ_1 and κ_2 are the background-to-signal ratios measured by the two Atto425 fluorescence detectors. Overall, the tFCS curve is given by

$$g_2(\tau) = \{g_x(\tau)g_y(\tau)g_z(\tau)g_{\mathrm{ae}}(\tau) - 1\}g_{\mathrm{b}} \tag{3}$$

Polymer dynamics are incorporated into $g_2(\tau)$ through the statistics of r^t. The Rouse and Zimm models predict autocorrelation functions for this vector given by

$$\langle r^{t+\tau}\cdot r^t\rangle = \frac{6r_0^2}{\pi^2}\sum_{q=1}^{\infty}\frac{1}{q^2}e^{-\tau/\tau_q} \tag{4}$$

where τ_q is the relaxation time of mode q. This relaxation time depends on the relative strength of the hydrodynamic interactions, quantified by the dimensionless *draining parameter* h and given by[34] $\tau_q \approx (1+h)(q^2 + hq^{3/2})^{-1}\tau_1$, where τ_1 is the relaxation time of the first intramolecular mode ($q = 1$). This expression is approximate because the $q^{3/2}$ term is accurate only for large q; exact values are given in ref 34 for $q < 8$ (deviating up to 12% from $q^{-3/2}$) and are used in our fits. In the Rouse model $h = 0$, so $\tau_q = \tau_1 q^{-2}$. The Zimm model refers to the limit of very strong **HI**, $h \to \infty$ so that $\tau_q \approx \tau_1 q^{-3/2}$. We will fit for an intermediate model with h as a free parameter in addition to these limits, and we will consider the approximate form $\tau_q \approx \tau_1 q^{-4/3}$ for a semiflexible polymer even though the molecule under study is unperturbed and much longer than its persistence length (and hence appears essentially flexible[5,6,12]).

We determine all of the systematic parameters in the tFCS curve independently: we find σ and γ from $\hat{D}(\tau)$, we find w by scanning the probe beam over an immobilized fluorescent bead (see the Supporting Information), and we find κ_1 and κ_2 by measuring the background rate while tracking molecules with bleached probe dyes. As a result, our fits contain only two or three free parameters: r_0 and τ_1 alone for the Rouse and Zimm models and additionally h for the intermediate model. These parameters act on the tFCS curve in different ways: r_0 determines the variance $g_2(0)$, τ_1 determines the characteristic decay time, and h determines the steepness of the decay by spreading out (Rouse limit) or bunching together (Zimm limit) the normal mode decay times.

Figure 2 shows the tFCS curve measured from 763 s of fluorescence data from 58 different molecules. To suppress decays on long time scales (see the next section), the data was processed by breaking each tracking trajectory into 2 s intervals, computing the tFCS curve within each interval, and averaging

(33) Berglund, A. J.; Mabuchi, H. *Appl. Phys. B: Laser Opt.* **2006**, *83*, 127–133.

(34) Yamakawa, H. *Modern theory of polymer solutions*, electronic ed.; Harper & Row: New York, 1971.

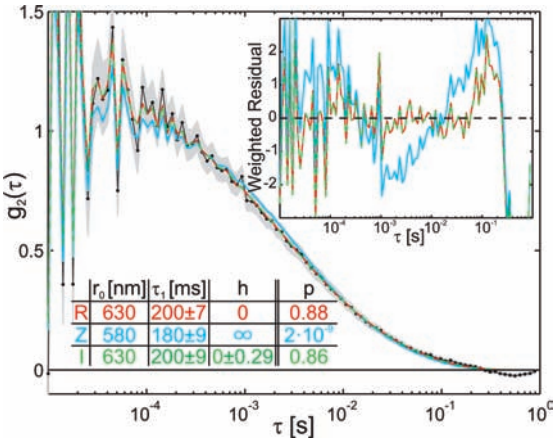

Figure 2. Measured tFCS curve (black circles) with 2σ confidence intervals (gray); weighted least-squares fit curves for the Rouse (red), Zimm (cyan), and intermediate (green) models are superimposed. (Inset) Residuals weighted by statistical uncertainty in the data. Table: fit parameters and χ^2 p values. Ninety-five percent confidence intervals are given for τ_1 and h, but the fitting uncertainty in r_0 is less than 1%, so the errors in r_0 are dominated by the beam waist calibration accuracy. Equation 4 was calculated by truncating the sum at $q = 1000$.

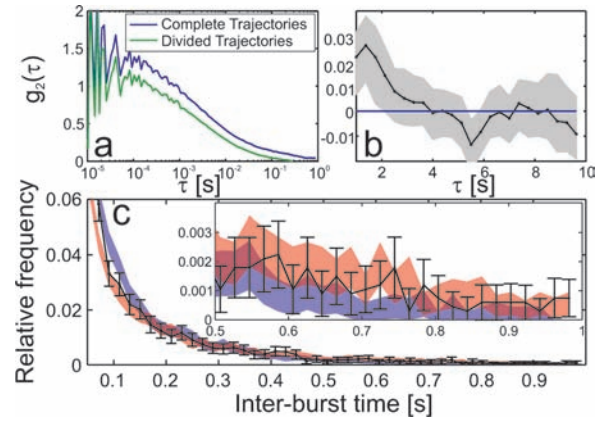

Figure 3. Evidence of long time-scale fluctuations. (a) Effect on tFCS curve of dividing trajectories into 2 s bins. (b) tFCS curve for $\tau > 1$ s for trajectories 10s or longer, with the 2σ uncertainty region shaded in gray. (c) Histogram of waiting times between fluorescence bursts for the data (black), for Rouse simulations with exponential dye blinking (blue), and for Rouse simulations with excluded volume interactions (red). Histograms are normalized so that their peaks have a value of 1. Ninety-five percent uncertainty intervals were calculated using the bootstrap method with 10^4 bootstrap samples. (Inset) Expanded view of the tail of the histograms.

the curves. The oscillations in the data for small τ are due to 240 kHz alternating excitation. The tFCS curve exhibits a small negative dip for $\tau > 200$ ms. This feature is not predicted by the Rouse or Zimm model nor by any other model describing highly damped intramolecular motion. We attribute it to an artifact in the response of the z axis of the tracking system, which has a slow bandwidth commensurate with this time scale and is sensitive to the complicated 3-dimensional geometry of the tracking beams.[35] We observed a similar dip in earlier data in ref 19 using the same instrument. Fortunately, this artifact is well separated from the polymer dynamics, as all fit curves are nearly zero on this time scale.

Weighted least-squares fits to eq 3 for 10 μs $< \tau <$ 100 ms were performed in MATLAB (The MathWorks, Natick, MA) for the Rouse, Zimm, and intermediate models. The fitted values for r_0 are in close agreement at $r_0 \approx 600$ nm. We infer the radius of gyration from this value, which for either polymer model is given by $R_g = r_0/\sqrt{2} \approx 420$ nm. Assuming the relationship between R_g and D given by the Kirkwood−Riseman theory,[36] $D \approx k_B T/4\pi\eta R_g$, this value for R_g is consistent with a room-temperature diffusion coefficient in water $D \approx 0.8$ μm^2/s, in accordance with our measurement from the tracking stage statistics. This approximation accounts for hydrodynamic interactions, so that our measured D and r_0 are consistent with these interactions dominating the center-of-mass motion.

The fit values for τ_1 are near 200 ms for all three models. The Rouse and Zimm models give predictions that relate τ_1 to other dynamical quantities: Rouse predicts $\tau_1 = r_0^2/\pi^2 D = 50$ ms and Zimm predicts $\tau_1 \approx 0.19 r_0^2/D = 82$ ms[3]. Our measured values for τ_1, r_0, and D are therefore not internally consistent with either model but are off by only a small factor in both cases.

The goodness-of-fit was evaluated by calculating the sum of squares of the uncertainty-weighted residuals. We assume that the measurement noise is Gaussian and compute p values from the χ^2 distribution. As indicated by $p = 2 \times 10^{-9}$, the Zimm model does not provide an acceptable fit to the tFCS data. Its relatively gradual decay underpredicts the data for $\tau < 500$ μs and $\tau > 10$ ms and overpredicts in between. By contrast, the Rouse predictions follow the data well over the entire fit range. The fit to the intermediate model yielded no significant improvement: given the constraint $h \geq 0$, the solver chose the Rouse value. In addition, we fit a curve for a semiflexible chain to the data (not shown in the figure). This curve closely resembles the Zimm one but with a more gradual decay, and this provided the worst fit to the data ($p = 10^{-25}$).

Long Time-Scale Dynamics. Our data contains slow fluctuations in the fluorescence intensity that cannot be explained by the Rouse or Zimm models (as in Figure 2, those models predict $g_2(\tau) \approx 0$ for $\tau > 300$ ms). In the previous section these were suppressed by dividing the trajectories into intervals over which the fluctuations were nearly constant. Here, we examine the data without dividing the trajectories in order to characterize the slow fluctuations.

Figure 3 demonstrates the presence of fluctuations on long time-scales. Figure 3a shows that dividing the trajectories into smaller intervals before computing the tFCS curve suppresses a significant offset, indicating correlations on time scales near or longer than the interval time (2 s in this case). Figure 3b shows the tFCS curve for $\tau > 1$ s, the prominent feature of which is a decay spanning, roughly, 2 s $< \tau <$ 5 s. This slow decay was absent in our measurements on identical molecules with multiple tFCS labels,[20] suggesting it is a consequence of the increased sensitivity to either intramolecular motion or dye photophysics afforded by the use of a single probe dye. An order of magnitude longer than the duration of a typical fluorescence burst, the time scale of this decay is poorly suited to analysis by tFCS because of the low degree of statistical correlation between adjacent burst pairs. An alternative approach is to compute the histogram of waiting times between fluorescence bursts in the tracking data. This distribution is sensitive to the number of dyes in the sample, dye photophysics, and dynamics of the dyes outside the focus of the laser. In our experiments there is exactly one Atto425 dye on each molecule, so that the interburst times reveal combined photophysical and conformational fluctuations.

(35) McHale, K. L. Ph.D. thesis, California Institute of Technology, 2008.
(36) Strobl, G. *The Physics of Polymers*; Springer-Verlag: Berlin, Heidelberg, 2007.

Figure 3c shows the histogram of the measured interburst waiting times. For comparison, we simulated Rouse data using the polymer parameters determined in the previous section and including exponential fluorophore blinking using the on and off rates found from the tFCS curves in Figure 3a and 3b according to $k_{off}/k_{on} = (g_1(0) + 1)/(g_0(0) + 1) - 1$, where g_1 and g_0 are the tFCS curves with and without the long-time contribution, respectively, and $k_{off} + k_{on} \approx 0.5\ s^{-1}$ (yielding $k_{on} \approx 0.39\ s^{-1}$ and $k_{off} \approx 0.11\ s^{-1}$). We varied the burst threshold in order to match the simulated waiting time histogram to that from the data, finding that the simulated histogram decays to zero faster than the measured one.

We expect our measurements to be sensitive to the 3-dimensional shape of the molecule because polymer configurations with the dye closer to the molecule's center of mass will produce brighter fluorescence than configurations with the dye further away. Large-scale changes in the molecule's shape occur more slowly than predicted by the Rouse or Zimm model because those "phantom chain" models allow the polymer to intersect itself. A potential source of the slow fluctuations is therefore the large-scale relaxation of the molecule's shape. We investigated this possibility by simulating a Rouse chain with excluded volume interactions labeled and tracked as in our experiment (simulation details are provided in the Supporting Information). The interburst waiting time distribution for this simulation is compared with the data and the Rouse/blinking model in Figure 3c, showing that the excluded volume simulation reproduces the data's more gradual decay to zero. We should note that neither simulation provided an acceptable overall fit to the data because of disagreement for short time delays; however, the relatively low fluorescence count rate limited the available threshold values to small integers and therefore limited the quality of the fit. Additionally, we note that the excluded volume simulation does not reproduce the long time scale tFCS decay, in contrast to the simulation with blinking in which the decay is present by construction.

Discussion

Literature values for the diffusion coefficient of genomic λ-phage DNA are in disagreement. Fluorescence microscopy yielded $0.47 \pm 0.01\ \mu m^2/s$,[37] which the authors corrected to $0.59 \pm 0.04\ \mu m^2/s$ to achieve consistency with dynamic light scattering;[38] FCS yielded $1.1\ \mu m^2/s$,[10,12] and electro-osmotic trapping yielded $0.32 \pm 0.02\ \mu m^2/s$.[14] Our measured value, $0.80 \pm 0.05\ \mu m^2/s$, falls between those of microscopy and FCS. Although the addition of intercalating labels has the potential to affect the molecule's diffusion coefficient, our measurements have a comparable label density to those of refs 10 and 12 and yet we find a smaller diffusion coefficient. Furthermore, we never observed significant diffusion coefficient variability in our own experiments over a wide range of label densities. The POPO-3 dye also introduces the possibility of light-induced DNA fragmentation,[39] but our measurement conditions minimize this effect: the peak excitation intensity of $\sim 100\ W/cm^2$, lower label density, and shorter sequences ensure that our molecules absorb optical energy at a rate approximately 10 000 times smaller than in ref 40, and in addition the imaging agent β-mercaptoethanol greatly reduces the rate of DNA photocleavage by intercalating dyes.[39] Photocleavage was observed after $\sim$100 ms in ref 40, so we expect our DNA molecules to remain intact for far longer than our longest (55 s) tracking period.

Unlike alternative techniques, our instrument directly measures the position of individual molecules using externally calibrated capacitive sensors. Furthermore, our diffusion coefficient estimation procedure is insensitive to the molecule's internal dynamics, and the molecule's freedom to move in three dimensions ensures that its motion is not biased by interactions with the sample cell as in ref 14. We therefore believe ours to be the best measurement of D for this molecule. The significant difference between it and previous values may be due to either bias or calibration inaccuracy, both of which are known difficulties with these methods.[41,42] In addition, it is possible that prior diffusion coefficient estimates were spuriously influenced by intramolecular motion, which was not accounted for in ref 37 and is difficult to isolate from translational motion in FCS. Intramolecular motion-induced bias of diffusion coefficient estimates will depend on molecular size because it is easier to detect such motion on larger molecules. This size-dependent bias could significantly affect experimentally determined diffusion coefficient scaling relationships, which are commonly measured in polymer studies.[13,37,38,43,44] Our results suggest the immediate importance of re-examining these relationships, particularly for larger dsDNA molecules; measurements spanning a wide range of dsDNA lengths are well within our present technical capabilities and will be pursued in the future.

A number of recent studies using FCS[10−13] or image correlation analysis for molecules immobilized in an electro-osmotic trap[14] have looked for signatures of hydrodynamic interactions in the fluorescence statistics of labeled dsDNA. The conclusions of these measurements were not consistent, with one finding the absence of HI in the intramolecular dynamics[11] and the remainder finding strong HI. Several of these studies used classical approximations from dynamic light scattering[45,46] in place of the true Rouse and Zimm dynamics. These approximations require[3] (i) $\tau \ll \tau_1$, partly to justify approximating the sum in eq 4 by an integral, and (ii) that the scattering angle k is large—in our notation, $k \gg (Dr_0^2\tau)^{-1/4}$. FCS generally violates both requirements: the Gaussian excitation beam acts as a filter that only admits fluctuations with small scattering angles[47] and, hence, long decay times. In the particular case of dsDNA, these approximations introduce significant errors within the time scales of the intramolecular correlation decay. The conclusions of refs 10 and 14 rely on both assumptions and so are difficult to interpret. In addition, the conclusions of ref 14 relied on oversimplified calculations of the fluorescence statistics of trapped objects.[20] Reference 11 relies on the first assumption and neglects the center-of-mass motion on short time scales; reanalysis of the original data using the exact Rouse and Zimm dynamics found evidence in support of *strong* HI.[16] Given this alternative conclusion, the fact that refs 12 and 13 evaluated

(37) Smith, D. E.; Perkins, T. T.; Chu, S. *Macromolecules* **1996**, *1996*, 1372–1373.
(38) Sorlie, S. S.; Pecora, R. *Macromolecules* **1990**, *2*, 487–497.
(39) Åkerman, B.; Tuite, E. *Nucleic Acids Res.* **1996**, *24*, 1080–1090.
(40) Lyon, W. A.; Fang, M. M.; Haskins, W. E.; Nie, S. *Anal. Chem.* **1998**, *70*, 1743–1748.
(41) Dertinger, T.; Pacheco, V.; von der Hocht, I.; Hartmann, R.; Gregor, I.; Enderlein, J. *ChemPhysChem* **2007**, *8*, 433–443.
(42) Berglund, A. J.; McMahon, M. D.; McClelland, J. J.; Liddle, J. A. *Opt. Express* **2008**, *16*, 14064–14075.
(43) Crick, S. L.; Jayaraman, M.; Frieden, C.; Wetzel, R.; Pappu, R. V. *Proc. Natl. Acad. Sci. U.S.A.* **2006**, *103*, 16764–16769.
(44) Robertson, R. M.; Laib, S.; Smith, D. E. *Proc. Natl. Acad. Sci. U.S.A.* **2006**, *103*, 7310–7314.
(45) de Gennes, P.-G. *Physics* **1967**, *3*, 37–45.
(46) Dubois-Violette, E.; de Gennes, P.-G. *Physics* **1967**, *3*, 181–198.
(47) Rička, J.; Binkert, T. *Phys. Rev. A* **1989**, *39*, 2646–2652.

the polymer models exactly and the longstanding theoretical consensus on this issue,[3] our determination that the Zimm model is a poor fit to the intramolecular component of our data comes as a very surprising result (although consistent with the original conclusions of the authors of ref 11). We must acknowledge that our use of intercalating labels for tracking presents the possibility of affecting the intramolecular dynamics when compared to refs 11 and 13; however, this should only affect the quantitative values of parameters, not the general nature of the polymer dynamics. In addition, ref 10 estimated that a label density comparable to ours has only a small effect, increasing the dsDNA persistence length by ~2%.

A question that has never been raised in these model discrimination experiments is how sensitive the measurements are to the differences between the predictions of different polymer models. In order to confirm the consistency of the data exclusively with one particular model, there must not exist any set of parameters under which the predictions of a competing model satisfy statistical goodness-of-fit tests. We found that this is not so with nontracking FCS measurements on the λ-phage DNA molecule.

We performed a numerical experiment to determine whether it would be possible to reject the Zimm model for experimental data consisting of Rouse FCS curves with additive, zero-mean Gaussian white noise. We computed Rouse FCS curves using our measured parameters both for end-labeled molecules and for molecules labeled homogeneously along their backbone (as in refs 10, 12, and 14). We performed least-squares fits of the Zimm model to these curves, weighted by appropriate noise standard deviations from our measurements. The expected value of the χ^2 statistic in this experiment is

$$\langle \chi^2 \rangle = N + \sum_n \sigma_n^{-2} [g_R(\tau_n) - g_Z^*(\tau_n)]^2 \qquad (5)$$

where $g_R(\tau_n)$ and $g_Z^*(\tau_n)$ are the Rouse and best-fit Zimm curves at lag times τ_n and σ_n^2 are measurement variances. We calculated $\langle \chi^2 \rangle$ as a function of σ_1, fixing the ratios between the σ_n to those from our measurements, and transformed the results into p values representing the goodness of the expected fit to the data. For continuous labeling, $g_Z^*(\tau)$ was nearly indistinguishable from $g_R(\tau)$, and a measurement noise of $\sigma_1 < 0.7\%$ at a lag time of 10 μs was required to reject the Zimm model with 95% confidence on average. The curves were less similar in the end-labeled case, requiring $\sigma_1 < 7\%$ at 10 μs.

Our measurements in this paper had a standard deviation of about 7% at 10 μs from 763 s of data taken on constantly illuminated molecules (repeated 7 s are a coincidence). In a polymer FCS experiment the sample concentration must be kept low to reduce the intermolecular overlap probability.[13] If we assume, probably conservatively, that our experiment enhances the rate at which we collect fluorescence information by a factor of 10 over a dilute sample, then we would require 200 h of data to reject the Zimm model in the continuous labeling case and 2 h of data in the end-labeled case. While such measurement times are attainable, it is important to note that we assumed that all experimental parameters remain constant over the entire measurement. Photobleaching and surface adsorption inevitably reduce the effective sample concentration over time, while laser intensity drifts add additional noise if not corrected experimentally. These factors all increase the measurement uncertainty, making it more difficult to reject the inappropriate model. We therefore conclude that without extreme experimental precision it *is not possible* to distinguish between Rouse and Zimm dynamics in an FCS experiment.

Tracking-FCS is more discriminative than FCS because it is insensitive to sample concentration, and it is much less sensitive to the molecule's diffusion coefficient. In addition, it is more sensitive to the molecule's size parameter r_0, which alone determines the variance $g_2(0)$ by defining an effective concentration of dyes within the molecule.[20] By contrast, r_0 has no effect on $g_2(0)$ in FCS. As a result, the two free parameters in the tracking-FCS curve are nearly orthogonal to each other, while three free parameters in the ordinary FCS curve (r_0, τ_1, and D) overlap to define the shape of the decay, and a fourth parameter (the concentration) provides an overall scale factor. With twice as many free parameters, it is not surprising that the FCS curve is underdetermined and the tFCS curve is not.

We must stress that while our intramolecular measurements are not consistent with the Zimm model, neither do they prove that the Rouse model is an appropriate description of the polymer's motion. Our measurements of r_0 and D are together consistent with strong HI, and the Zimm model is closer than the Rouse model by about a factor of 2 in predicting τ_1 from those numbers. The differences between our data and the Zimm model are primarily in the finer structure of the correlation decay, as determined by the mode spacing of the time constants τ_q. Predicting an even narrower spacing between τ_q, the semiflexible chain model yielded the poorest fit to the data; this is not surprising, however, because the bending modes of such a large molecule are dominated by the stretching modes characteristic of flexible polymers.[5,6,12] A modification of the Zimm model that incorporates excluded volume interactions has been proposed,[3] but we found it to have little effect on the tFCS curves, and its validity has been a subject of criticism.[48] It has been shown that a (small[34]) correction to the Fourier eigenbasis for the Zimm model produces FCS curves that are more Rouse-like in their decay,[49] suggesting a potential area for improvement of our fits. However, the fact that we cannot reject the Rouse model implies that any further study will require better measurements, possibly achievable with FRET or other techniques that provide the sensitivity required to probe polymer motion on fine spatial scales.

We have not come to a definitive conclusion on the nature of the slow fluctuations in our measurements. While neither the blinking model nor the excluded volume model provided a satisfactory overall fit to the waiting time distribution, other aspects of our measurements are not consistent with significant blinking on the 2 s time scale. According to the estimated on-rate $k_{on} = 0.39\ s^{-1}$, about 31% of off periods would be expected to last 3 s or longer. Together k_{on} and $k_{off} = 0.11\ s^{-1}$ predict that among our 763 s of data we should expect to observe about 65 off periods and hence 20 ± 7 lasting longer than 3s; however, we observe only 7 off periods (determined using a threshold of 5 photons in 1 ms to prevent background counts from reducing this number) lasting this long. Instead, qualitatively the data appears to contain slow drifts in the overall fluorescence intensity with no clear trends over time. The data in Figure 1 exhibits this characteristic, with several periods dense with fluorescence bursts separated by much sparser periods (for more examples, every tracking trajectory used in our analysis is

(48) Prakash, J. R. *Macromolecules* **2001**, *34*, 3396–3411.
(49) Hinczewski, M.; Schlagberger, X.; Rubinstein, M.; Krichevsky, O.; Netz, R. R. *Macromolecules* **2009**, *42*, 860–875.

displayed in the Supporting Information). The possibility that these fluctuations arise from slow conformational rearrangement of the molecule is intriguing, but our best evidence in support of this hypothesis is the longer tail in the simulated waiting time histogram. The absence of the slow decay in the tFCS curve of the simulated data is not surprising given that the simulation parameters were not tuned to values appropriate to dsDNA. To convincingly determine whether conformational fluctuations can explain the slow fluctuations in our data will require both more detailed theoretical work and further experimental study aimed at ruling out other systematic possibilities.

Conclusion

We presented the most sensitive study of the dynamics of a large flexible polymer to date and have come to surprising conclusions. Our measurements revealed a disconnect between the nature of the center-of-mass and intramolecular motion of the molecule with the former dominated by hydrodynamic interactions and the latter inconsistent with the Zimm model. We addressed technical limitations of prior studies that generated inconsistent values for this molecule's diffusion coefficient and drew conclusions regarding the nature of the intramolecular dynamics based on measurements that likely lacked sufficient sensitivity to do so. Finally, we detected previously undocumented fluorescence fluctuations over long time scales and identified a potential physical mechanism for their source that will be investigated in future studies.

The advances in this paper were made possible by enhancements that come as a subtle consequence of combining feedback tracking with FCS. Tracking-FCS is uniquely well suited to the study of large polymers because it is simultaneously more sensitive to the intrinsic properties of the polymer and less sensitive to extrinsic and systematic variables than FCS and other related techniques. The results in this paper demonstrate the quantitative precision of this technique and the value of the measurements it enables with long per-molecule observation times.

Acknowledgment. We thank Aaron Straight and Colin Fuller for suggestions on DNA labeling and purification methods and Michael Zhang for suggestions that improved this manuscript.

Supporting Information Available: Details on sample preparation, experimental apparatus, and simulations; details on tracking fluorescence intensity control loop; fits to data for $\hat{D}(\tau)$; derivation of $g_{ae}(\tau)$; derivation of tracking errors induced by alternating excitation; probe beam focal geometry determination; plots of all fluorescence data used in the analysis. This material is available free of charge via the Internet at http://pubs.acs.org.

JA906979J